Cite as: H. Nishimasu *et al.*, *Science* 10.1126/science.aas9129 (2018).

Engineered CRISPR-Cas9 nuclease with expanded targeting space

Hiroshi Nishimasu[1]*, Xi Shi[2,3], Soh Ishiguro[4,5,6], Linyi Gao[2,7], Seiichi Hirano[1], Sanae Okazaki[1], Taichi Noda[8], Omar O. Abudayyeh[2,3,9], Jonathan S. Gootenberg[2,3,9], Hideto Mori[4,5,6], Seiya Oura[8], Benjamin Holmes[2,3], Mamoru Tanaka[4], Motoaki Seki[4], Hisato Hirano[1], Hiroyuki Aburatani[4], Ryuichiro Ishitani[1], Masahito Ikawa[8], Nozomu Yachie[1,4,5,6], Feng Zhang[2,3,7,9], Osamu Nureki[1]*

[1]Department of Biological Sciences, Graduate School of Science, University of Tokyo, 7-3-1 Hongo, Bunkyo-ku, Tokyo 113-0033, Japan. [2]Broad Institute of MIT and Harvard, Cambridge, MA 02142, USA. [3]McGovern Institute for Brain Research, Cambridge, MA 02139, USA. [4]Research Center for Advanced Science and Technology, University of Tokyo, 4-6-1 Komaba, Meguro-ku, Tokyo 153-8904, Japan. [5]Institute for Advanced Biosciences, Keio University, 14-1 Baba-cho, Tsuruoka, Yamagata 997-0035, Japan. [6]Graduate School of Media and Governance, Keio University, 5322 Endo, Fujisawa, Kanagawa 252-0882, Japan. [7]Department of Biological Engineering, Massachusetts Institute of Technology, Cambridge, MA 02139, USA. [8]Research Institute for Microbial Diseases, Osaka University, 3-1 Yamadaoka, Suita, Osaka 565-0871, Japan. [9]Department of Brain and Cognitive Sciences, Massachusetts Institute of Technology, Cambridge, MA 02139, USA.

*Corresponding author. Email: nisimasu@bs.s.u-tokyo.ac.jp (H.N.); nureki@bs.s.u-tokyo.ac.jp (O.N.)

The RNA-guided endonuclease Cas9 cleaves its target DNA and is a powerful genome-editing tool. However, the widely used *Streptococcus pyogenes* Cas9 enzyme (SpCas9) requires an NGG protospacer adjacent motif (PAM) for target recognition, thereby restricting the targetable genomic loci. Here, we report a rationally engineered SpCas9 variant (SpCas9-NG) that can recognize relaxed NG PAMs. The crystal structure revealed that the loss of the base-specific interaction with the third G is compensated by newly introduced non-base-specific interactions, enabling the NG PAM recognition. We showed that SpCas9-NG induces indels at endogenous target sites bearing NG PAMs in human cells. Furthermore, we found that the fusion of SpCas9-NG and the activation-induced cytidine deaminase (AID) mediates the C-to-T conversion at target sites with NG PAMs in human cells.

The CRISPR RNA-guided endonuclease Cas9 cleaves double-stranded DNA targets complementary to the RNA guide (*1*) (fig. S1), and has been harnessed for genome editing in eukaryotic cells (*2*). However, the widely used Cas9 from *Streptococcus pyogenes* (SpCas9) strictly recognizes an NGG sequence as the protospacer adjacent motif (PAM) (*3*), thereby restricting the targetable genomic loci. To address this limitation, structure-guided directed evolution approaches yielded several SpCas9 variants with altered PAM specificities, such as the SpCas9 VQR and VRER variants, which recognize the NGA and NGCG PAMs, respectively (*4*). In addition, Cas9 and Cas12a (also known as Cpf1) enzymes with distinct PAM specificities, such as *Staphylococcus aureus* Cas9 (SaCas9) (*5*), *Acidaminococcus sp*. Cas12a (AsCas12a) and *Lachnospiraceae bacterium* Cas12a (LbCas12a) (*6*), have extended the targeting range in CRISPR-Cas-mediated genome editing.

To expand the targeting range of CRISPR-Cas9, we sought to engineer an SpCas9 variant with relaxed preferences for the third nucleobase of the PAM. Previous studies revealed that the second and third G nucleobases in the NGG PAM are recognized by Arg1333 and Arg1335 of SpCas9, respectively (*7*) (fig. S2). We thus hypothesized that the PAM constraint can be reduced by eliminating the base-specific interaction between Arg1335 and the third G, and compensating for the loss of this base-specific interaction by introducing non-base-specific interactions with the PAM duplex. We first measured the in vitro cleavage activities of purified wild-type (WT) SpCas9 and the R1335A mutant toward a target plasmid with the TGG PAM, and confirmed that, whereas WT SpCas9 efficiently cleaves the TGG target, R1335A has almost no activity (fig. S3, A to C).

We next examined whether the R1335A activity is restored by the substitution of residues surrounding the PAM duplex, and found that the replacements of Leu1111, Gly1218, Ala1322 and Thr1337 with arginine partially restored the activity of the R1335A mutant (fig. S3, A to C). Furthermore, the R1335A/L1111R/G1218R/A1322R/T1337R variant (referred to as ARRRR) efficiently cleaved the TGG target (fig. S3, A to C). However, the cleavage kinetics of ARRRR was slower than that of WT SpCas9 (fig. S3, D and E). In the previously reported VQR and VRER variants, the D1135V mutation provides interactions with the sugar-phosphate backbone of the PAM duplex (*8*, *9*). In addition, molecular modeling suggested that the E1219F mutation forms hydrophobic interactions with the ribose moiety of the second G, and that the R1335V mutation stabilizes Arg1333 and Phe1219 (E1219F) (fig. S3F). Indeed, the addition of the

D1135V, E1219F and R1335V mutations enhanced the cleavage activity (fig. S3, D and E). We designated the R1335V/L1111R/D1135V/G1218R/E1219F/A1322R/T1337R variant as VRVRFRR.

We next examined the cleavage activities of VRVRFRR toward the target plasmid with TGN PAMs. As compared to WT SpCas9, VRVRFRR slowly but more efficiently cleaved the TGA, TGT and TGC targets (Fig. 1, A to C, and fig. S4). Although VRVRFRR is less active than WT SpCas9 and SaCas9, its cleavage activity was comparable to those of AsCas12a and LbCas12a (*5*, *6*) (fig. S5). Using an in vitro PAM identification assay (*10*), we confirmed that whereas WT SpCas9 is specific to NGG PAMs, VRVRFRR preferentially recognizes NG PAMs (Fig. 1D and fig. S6). Although the PAM identification assay revealed that VRVRFRR slightly recognizes NAN PAMs (Fig. 1D), in vitro cleavage experiments demonstrated that VRVRFRR is less active toward TAN PAMs relative to TGN PAMs (fig. S7). Thus, we concluded that VRVRFRR recognizes a relaxed PAM, and refer to this variant as SpCas9-NG, as it has increased activity on NGH PAMs, albeit with reduced relative activity on NGC.

We compared SpCas9-NG with the xCas9 enzyme (an SpCas9 variant with the A262T/R324L/S409I/E480K/E543D/M694I/E1219V mutations), which was engineered via directed evolution and recognizes NG PAMs (*11*) (fig. S8). We measured their in vitro cleavage activities toward the target plasmid with the TGN PAMs. Under our assay conditions (50 nM Cas9), xCas9 showed almost no activities toward the TGA, TGT and TGC targets, while it cleaved the TGG target with lower efficiency as compared to that of SpCas9-NG (Fig. 1, A to C and E, and fig. S9A). At a higher concentration (200 nM Cas9), xCas9 cleaved the TGA, TGT and TGC targets (fig. S9, D and G); nonetheless, the cleavage kinetics of xCas9 was slower than that of SpCas9-NG (fig. S9, C, D, F, and G), and the cleavage activities of xCas9 toward the TGT and TGA/TGC targets were comparable to or lower than that of WT SpCas9 toward the non-canonical TGA target, respectively (fig. S9, B, D, E, and G). These results demonstrated that SpCas9-NG outperforms xCas9 in recognizing NGH PAMs in vitro.

To clarify the NG PAM recognition mechanism, we determined the 2.7 Å-resolution crystal structure of SpCas9-NG in complex with an sgRNA and its target DNA containing the TGG PAM (fig. S10A and table S1). The second G in the PAM (dG2*) forms bidentate hydrogen bonds with Arg1333 (Fig. 2A), which is stabilized by Val1335 (R1335V). The third G (dG3*) forms a hydrogen bond with Arg1337 (T1337R) (Fig. 2A), consistent with the preference of SpCas9-NG for the third G (Fig. 1C). Arg1111 (L1111R), Val1135 (D1135V) and Phe1219 (E1219F) interact with the sugar-phosphate backbone of the PAM duplex, while Arg1218 (G1218R) does not directly interact with the DNA backbone (Fig. 2B). A structural comparison with the SpCas9 R-loop complex (*12*) suggested that Arg1322 (A1322R) interacts with the non-target DNA strand (fig. S10B).

To assess the activity of SpCas9-NG in mammalian cells, we next measured the indel formation induced by WT SpCas9, SpCas9-NG and xCas9 at 69 endogenous target sites with NGN PAMs in HEK293FT cells (table S2). As expected, WT SpCas9 induced indels predominately at the NGG sites, with some recognition of NGA sites (Fig. 3, A and B). WT SpCas9 achieved >20% indel at NGG (17 out of 17 sites) and NGA sites (3 out of 19 sites), but not NGT (0 out of 18 sites) and NGC (0 out of 15 sites) sites (Fig. 3, A and B). In contrast, SpCas9-NG edited NGA, NGT and NGG sites, with lower activity at NGC (Fig. 3, A and B), consistent with the in vitro cleavage preference for the third D (not C) PAM nucleotide (Fig. 1C). SpCas9-NG achieved >20% indel at 13 NGG, 13 NGA, 15 NGT and 5 NGC sites (Fig. 3, A and B). xCas9 had lower editing efficiency at all of the NGH sites, as compared to SpCas9-NG (Fig. 3, A and B), consistent with our in vitro cleavage data (Fig. 1E). xCas9 induced >20% indel at 15 NGG, 5 NGA and 4 NGT, but none at NGC sites (Fig. 3, A and B).

Using GUIDE-seq (*13*), we examined the specificity of WT SpCas9 and SpCas9-NG in human cells at two previously characterized target sites (*EMX1* and *VEGFA*). We found that WT SpCas9 and SpCas9-NG have comparable numbers of off-target sites for the *EMX1* target, and that the high-fidelity mutations in eSpCas9(1.1) (K848A/K1003A/R1060A) (*14*) substantially reduced the off-target cleavage by SpCas9-NG (Fig. 3C and fig. S11). These results demonstrated that SpCas9-NG has cleavage specificity comparable to that of WT SpCas9, and that its specificity can be enhanced by the high-fidelity mutations. As expected, SpCas9-NG had a different off-target profile with off-target sites harboring NGH PAMs (fig. S11), further confirming the relaxed PAM recognition.

The nuclease-inactive version of SpCas9 can be applied to numerous technologies, such as base editing (*15*, *16*). We examined whether the SpCas9-NG D10A nickase fused to the activation-induced cytidine deaminase (nSpCas9-NG–AID, referred to as Target-AID-NG) mediates C-to-T conversion at 32 endogenous target sites with NG PAMs in human cells (table S3). nSpCas9–AID (Target-AID) efficiently induced C-to-T conversion at the NGG sites, with lower activity at NGA sites and no activity at NGT/NGC sites (Fig. 4A and figs. S12A and S13). In contrast, Target-AID-NG showed base-editing activity toward all PAMs assessed, albeit with lower efficiency at NGC sites (Fig. 4A and figs. S12A and S13), consistent with the indel data (Fig. 3A). In addition, Target-AID-NG showed higher base-editing efficiencies than the xCas9 D10A nickase fused to the APOBEC1 cytidine deaminase (xCas9–BE4) at most of the tested poly-C-

containing on-target sites (Fig. 4B and figs. S12B and S13). These results demonstrate that the catalytically inactive version of SpCas9-NG can serve as a useful RNA-guided DNA targeting platform.

In this study, we engineered an SpCas9-NG variant with an increased targeting range (fig. S14). Nonetheless, the cleavage activity of SpCas9-NG is lower than that of WT SpCas9 at NGG sites, and SpCas9-NG is less active at NGC sites relative to NGD sites. Thus, it will be important to improve the activity of SpCas9-NG by further molecular engineering. Overall, the rationally designed SpCas9-NG and its high-fidelity variants can serve as useful genome-editing tools with increased versatility across genomes.

REFERENCES AND NOTES

1. M. Jinek, K. Chylinski, I. Fonfara, M. Hauer, J. A. Doudna, E. Charpentier, A programmable dual-RNA-guided DNA endonuclease in adaptive bacterial immunity. *Science* 337, 816–821 (2012). doi:10.1126/science.1225829 Medline
2. L. Cong, F. A. Ran, D. Cox, S. Lin, R. Barretto, N. Habib, P. D. Hsu, X. Wu, W. Jiang, L. A. Marraffini, F. Zhang, Multiplex genome engineering using CRISPR/Cas systems. *Science* **339**, 819–823 (2013). doi:10.1126/science.1231143 Medline
3. S. H. Sternberg, S. Redding, M. Jinek, E. C. Greene, J. A. Doudna, DNA interrogation by the CRISPR RNA-guided endonuclease Cas9. *Nature* **507**, 62–67 (2014). doi:10.1038/nature13011 Medline
4. B. P. Kleinstiver, M. S. Prew, S. Q. Tsai, V. V. Topkar, N. T. Nguyen, Z. Zheng, A. P. W. Gonzales, Z. Li, R. T. Peterson, J.-R. J. Yeh, M. J. Aryee, J. K. Joung, Engineered CRISPR-Cas9 nucleases with altered PAM specificities. *Nature* **523**, 481–485 (2015). doi:10.1038/nature14592 Medline
5. F. A. Ran, L. Cong, W. X. Yan, D. A. Scott, J. S. Gootenberg, A. J. Kriz, B. Zetsche, O. Shalem, X. Wu, K. S. Makarova, E. V. Koonin, P. A. Sharp, F. Zhang, *In vivo* genome editing using *Staphylococcus aureus* Cas9. *Nature* **520**, 186–191 (2015). doi:10.1038/nature14299 Medline
6. B. Zetsche, J. S. Gootenberg, O. O. Abudayyeh, I. M. Slaymaker, K. S. Makarova, P. Essletzbichler, S. E. Volz, J. Joung, J. van der Oost, A. Regev, E. V. Koonin, F. Zhang, Cpf1 is a single RNA-guided endonuclease of a class 2 CRISPR-Cas system. *Cell* **163**, 759–771 (2015). doi:10.1016/j.cell.2015.09.038 Medline
7. C. Anders, O. Niewoehner, A. Duerst, M. Jinek, Structural basis of PAM-dependent target DNA recognition by the Cas9 endonuclease. *Nature* **513**, 569–573 (2014). doi:10.1038/nature13579 Medline
8. C. Anders, K. Bargsten, M. Jinek, Structural plasticity of PAM recognition by engineered variants of the RNA-guided endonuclease Cas9. *Mol. Cell* **61**, 895–902 (2016). doi:10.1016/j.molcel.2016.02.020 Medline
9. S. Hirano, H. Nishimasu, R. Ishitani, O. Nureki, Structural basis for the altered PAM specificities of engineered CRISPR-Cas9. *Mol. Cell* **61**, 886–894 (2016). doi:10.1016/j.molcel.2016.02.018 Medline
10. L. Gao, D. B. T. Cox, W. X. Yan, J. C. Manteiga, M. W. Schneider, T. Yamano, H. Nishimasu, O. Nureki, N. Crosetto, F. Zhang, Engineered Cpf1 variants with altered PAM specificities. *Nat. Biotechnol.* **35**, 789–792 (2017). doi:10.1038/nbt.3900 Medline
11. J. H. Hu, S. M. Miller, M. H. Geurts, W. Tang, L. Chen, N. Sun, C. M. Zeina, X. Gao, H. A. Rees, Z. Lin, D. R. Liu, Evolved Cas9 variants with broad PAM compatibility and high DNA specificity. *Nature* **556**, 57–63 (2018). doi:10.1038/nature26155 Medline
12. F. Jiang, D. W. Taylor, J. S. Chen, J. E. Kornfeld, K. Zhou, A. J. Thompson, E. Nogales, J. A. Doudna, Structures of a CRISPR-Cas9 R-loop complex primed for DNA cleavage. *Science* **351**, 867–871 (2016). doi:10.1126/science.aad8282 Medline
13. S. Q. Tsai, Z. Zheng, N. T. Nguyen, M. Liebers, V. V. Topkar, V. Thapar, N. Wyvekens, C. Khayter, A. J. Iafrate, L. P. Le, M. J. Aryee, J. K. Joung, GUIDE-seq enables genome-wide profiling of off-target cleavage by CRISPR-Cas nucleases. *Nat. Biotechnol.* **33**, 187–197 (2015). doi:10.1038/nbt.3117 Medline
14. I. M. Slaymaker, L. Gao, B. Zetsche, D. A. Scott, W. X. Yan, F. Zhang, Rationally engineered Cas9 nucleases with improved specificity. *Science* **351**, 84–88 (2016). doi:10.1126/science.aad5227 Medline
15. A. C. Komor, Y. B. Kim, M. S. Packer, J. A. Zuris, D. R. Liu, Programmable editing of a target base in genomic DNA without double-stranded DNA cleavage. *Nature* **533**, 420–424 (2016). doi:10.1038/nature17946 Medline
16. K. Nishida, T. Arazoe, N. Yachie, S. Banno, M. Kakimoto, M. Tabata, M. Mochizuki, A. Miyabe, M. Araki, K. Y. Hara, Z. Shimatani, A. Kondo, Targeted nucleotide editing using hybrid prokaryotic and vertebrate adaptive immune systems. *Science* **353**, aaf8729 (2016). doi:10.1126/science.aaf8729 Medline
17. H. Nishimasu, L. Cong, W. X. Yan, F. A. Ran, B. Zetsche, Y. Li, A. Kurabayashi, R. Ishitani, F. Zhang, O. Nureki, Crystal Structure of *Staphylococcus aureus* Cas9. *Cell* **162**, 1113–1126 (2015). doi:10.1016/j.cell.2015.08.007 Medline
18. T. Yamano, B. Zetsche, R. Ishitani, F. Zhang, H. Nishimasu, O. Nureki, Structural basis for the canonical and non-canonical PAM recognition by CRISPR-Cpf1. *Mol. Cell* **67**, 633–645.e3 (2017). doi:10.1016/j.molcel.2017.06.035 Medline
19. W. Kabsch, XDS. *Acta Crystallogr. D* **66**, 125–132 (2010). doi:10.1107/S0907444909047337 Medline
20. P. R. Evans, G. N. Murshudov, How good are my data and what is the resolution? *Acta Crystallogr. D* **69**, 1204–1214 (2013). doi:10.1107/S0907444913000061 Medline
21. A. Vagin, A. Teplyakov, Molecular replacement with MOLREP. *Acta Crystallogr. D* **66**, 22–25 (2010). doi:10.1107/S0907444909042589 Medline
22. P. Emsley, K. Cowtan, Coot: Model-building tools for molecular graphics. *Acta Crystallogr. D* **60**, 2126–2132 (2004). doi:10.1107/S0907444904019158 Medline
23. P. D. Adams, P. V. Afonine, G. Bunkóczi, V. B. Chen, I. W. Davis, N. Echols, J. J. Headd, L.-W. Hung, G. J. Kapral, R. W. Grosse-Kunstleve, A. J. McCoy, N. W. Moriarty, R. Oeffner, R. J. Read, D. C. Richardson, J. S. Richardson, T. C. Terwilliger, P. H. Zwart, PHENIX: A comprehensive Python-based system for macromolecular structure solution. *Acta Crystallogr. D* **66**, 213–221 (2010). doi:10.1107/S0907444909052925 Medline
24. P. D. Hsu, D. A. Scott, J. A. Weinstein, F. A. Ran, S. Konermann, V. Agarwala, Y. Li, E. J. Fine, X. Wu, O. Shalem, T. J. Cradick, L. A. Marraffini, G. Bao, F. Zhang, DNA targeting specificity of RNA-guided Cas9 nucleases. *Nat. Biotechnol.* **31**, 827–832 (2013). doi:10.1038/nbt.2647 Medline

ACKNOWLEDGMENTS

We thank Arisa Kurabayashi for assistance with sample preparation, Takashi Yamano for Cas12a preparation, and Benjamin P. Kleinstiver and Keith Joung for assistance with GUIDE-seq. We thank the beamline scientists at BL41XU at SPring-8 for assistance with data collection. Funding: H.N. is supported by JST (JPMJPR13L8) and JSPS (26291010 and 15H01463). S.I. is supported by JSPS (16J06287). M.I. is supported by JSPS (17H01394). N.Y. is supported by NEDO (Genome Editing Program), AMED (17 g6110007h0002), JST (10814) and JSPS (18H02428). F.Z. is supported by the National Institutes of Health through NIMH (5DP1-MH100706 and 1R01-MH110049) and NIDDK (5R01DK097768-03), the New York Stem Cell, Simons, Paul G. Allen Family, and Vallee Foundations. F.Z. is a New York Stem Cell Foundation Robertson Investigator. M.I. and O.N. are supported by the Japan Agency for Medical Research and Development (AMED). O.N. is supported by the Council for Science, Technology and Innovation (CSTI), Cross-ministerial Strategic Innovation Promotion Program (SIP). Author contributions: H.N. designed the variants, performed in vitro cleavage experiments and determined the crystal structure; X.S., L.G., O.O.A., J.S.G., B.H. and F.Z. performed PAM screens, indel detection and GUIDE-seq analyses; S.I., H.M., M.T., M.S., H.A. and N.Y. performed base-editing analyses;

T.N., S.O. and M.I. performed indel detection; S.H. performed crystallization; H.N., S.H., S.O. and H.H. prepared the proteins; R.I. assisted with the structural determination; H.N. wrote the manuscript with help from all authors; H.N. and O.N. supervised the research. Competing interests: H.N. is a scientific advisor for EdiGENE. F.Z. is a co-founder and scientific advisor for Editas Medicine, Pairwise Plants, Beam Therapeutics, and Arbor Biotechnologies. F.Z. serves as a director for Beam Therapeutics and Arbor Biotechnologies. O.N. is a co-founder, board member and scientific advisor for EdiGENE. H.N., H.H. and O.N. have filed a patent application related to this work. Data and materials availability: The atomic coordinates of SpCas9-NG have been deposited in the Protein Data Bank, with the PDB code 5ZMH. All data are available in the manuscript or the supplementary material.

SUPPLEMENTARY MATERIALS

www.sciencemag.org/cgi/content/full/science.aas9129/DC1
Materials and Methods
Figs. S1 to S14
Tables S1 to S3
References (*17*–*24*)

4 January 2018; accepted 16 August 2018
Published online 30 August 2018
10.1126/science.aas9129

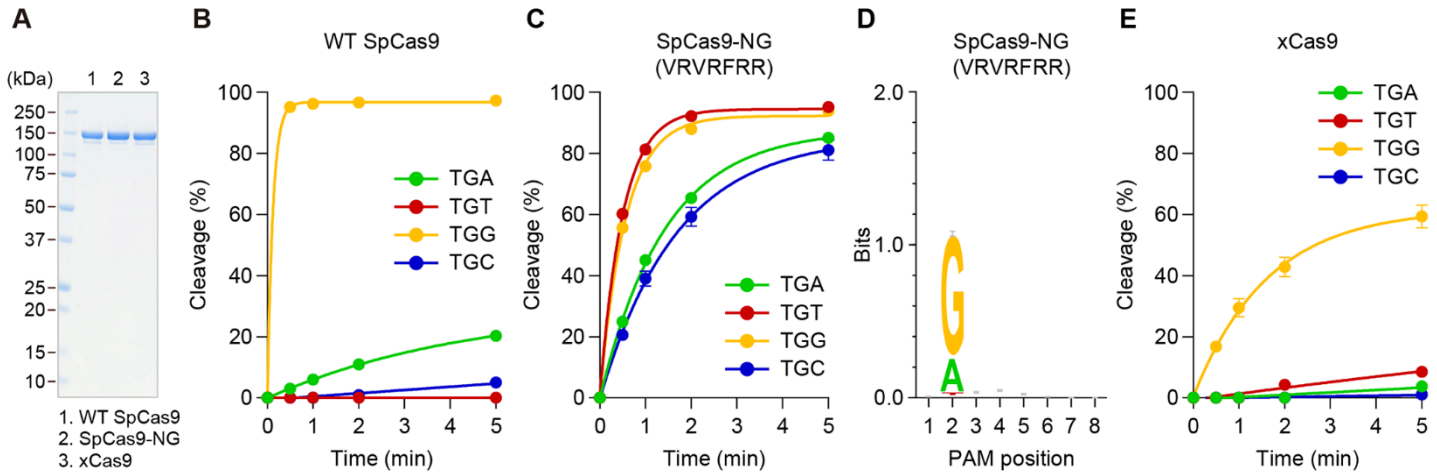

Fig. 1. In vitro cleavage activity. (**A**) SDS-PAGE analysis of WT SpCas9, SpCas9-NG and xCas9. (**B**, **C**, and **E**) In vitro DNA cleavage activities of WT SpCas9 (B), SpCas9-NG (C) and xCas9 (E) toward the TGN PAM targets. Data are means ± s.d. (*n* = 3). (**D**) PAM preference of SpCas9-NG.

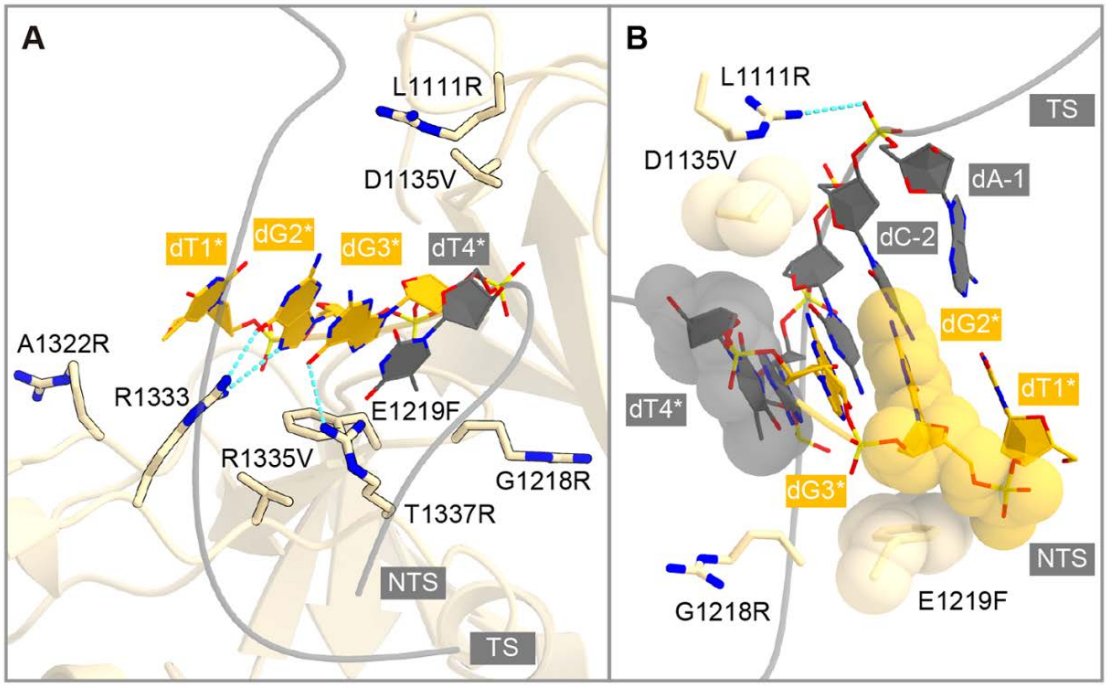

Fig. 2. Crystal structure of SpCas9-NG. (**A** and **B**) Recognition of the PAM duplex by SpCas9-NG.

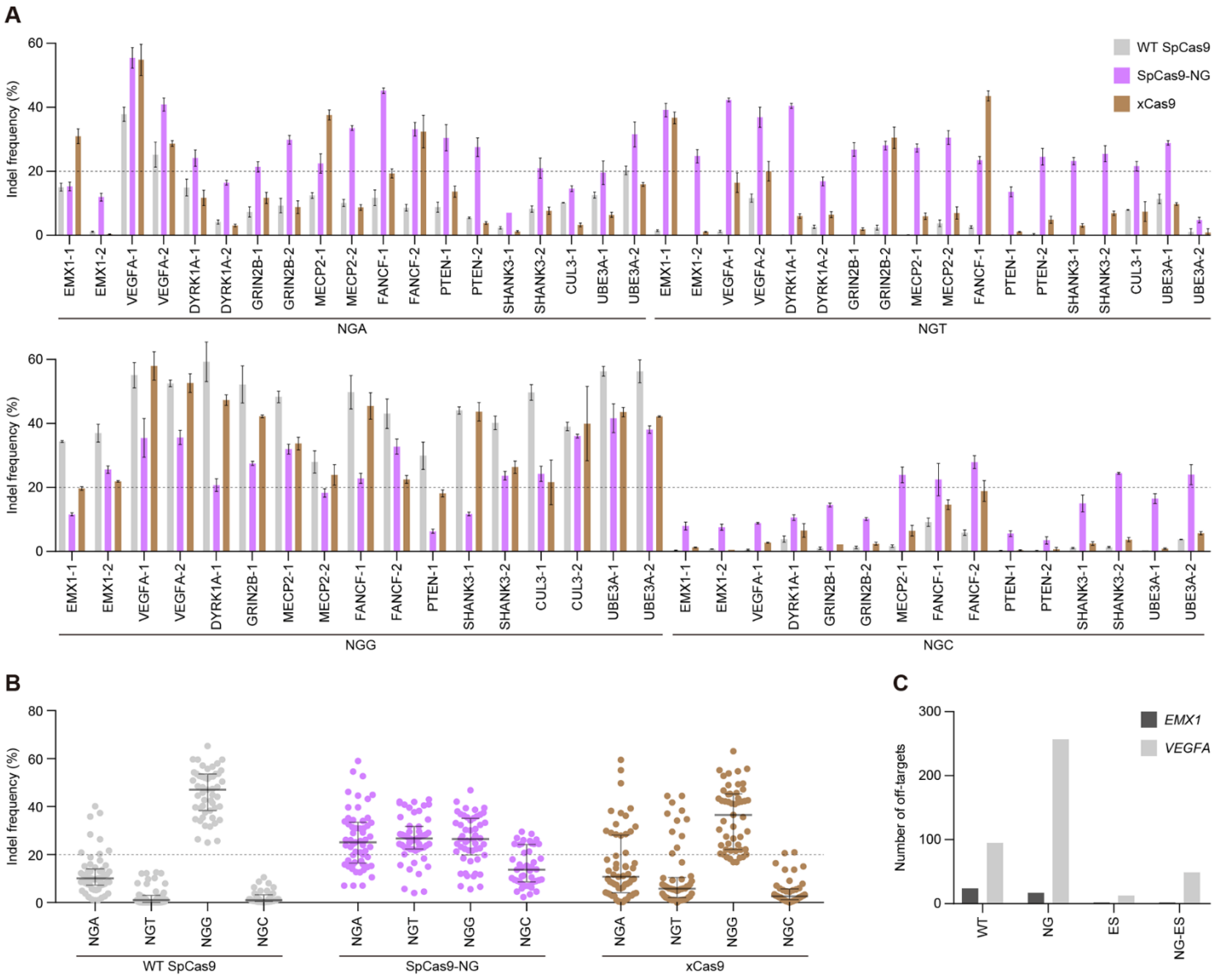

Fig. 3. Gene editing in human cells. (**A**) Indel formation efficiencies of WT SpCas9, SpCas9-NG and xCas9 at the 69 endogenous target sites in HEK293FT cells. Data are means ± s.d. (n = 3). (**B**) Summary of the editing efficiencies of SpCas9, SpCas9-NG and xCas9. Medians and first and third quartiles are shown. (**C**) Specificities of SpCas9 (WT), SpCas9-NG (NG), and the high-fidelity versions of SpCas9 (ES) and SpCas9-NG (NG-ES). The off-target cleavages were evaluated by GUIDE-seq.

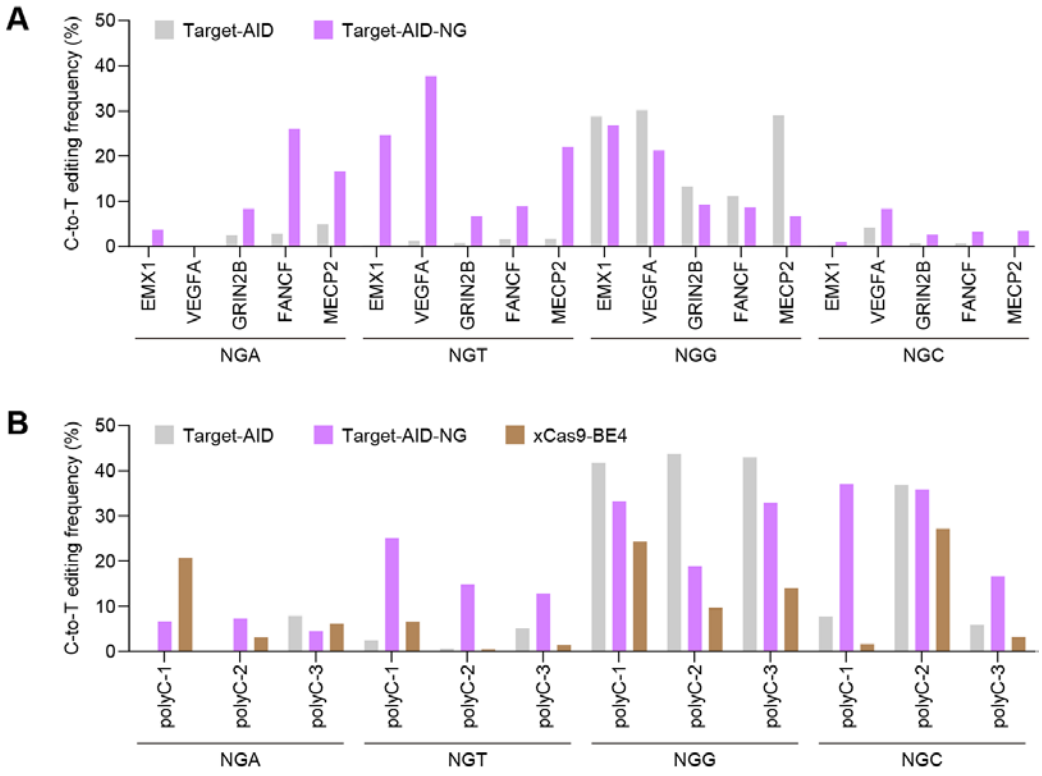

Fig. 4. Base editing in human cells. (**A** and **B**) C-to-T conversion efficiencies at the 20 endogenous target sites (Target-AID and Target-AID-NG) (A) and at the 12 poly-C-containing target sites (Target-AID, Target-AID-NG and xCas9-BE4) (B) in HEK293T cells. The experiments were performed at least twice, and similar results were obtained.

Engineered CRISPR-Cas9 nuclease with expanded targeting space

Hiroshi Nishimasu, Xi Shi, Soh Ishiguro, Linyi Gao, Seiichi Hirano, Sanae Okazaki, Taichi Noda, Omar O. Abudayyeh, Jonathan S. Gootenberg, Hideto Mori, Seiya Oura, Benjamin Holmes, Mamoru Tanaka, Motoaki Seki, Hisato Hirano, Hiroyuki Aburatani, Ryuichiro Ishitani, Masahito Ikawa, Nozomu Yachie, Feng Zhang and Osamu Nureki

published online August 30, 2018

Science (print ISSN 0036-8075; online ISSN 1095-9203) is published by the American Association for the Advancement of Science, 1200 New York Avenue NW, Washington, DC 20005.